

Improved Output Performance of High-Power VCSELs

Michael Miller and Ihab Kardosh

The intention of this paper is to report on state-of-the-art high-power vertical-cavity surface-emitting laser diodes (VCSELs), single devices as well as two-dimensional arrays. Both approaches are studied in terms of electro-optical characteristics, beam performance and scaling behavior. The maximum cw output power at room temperature of large-area bottom-emitting devices with active diameters up to 320 μm is as high as 0.89 W which is to our knowledge the highest value reported for a single device. Measurements under pulsed conditions show more than 10 W optical peak output power. Also the cw performance of two-dimensional arrays has been increased from 0.56 W for 23 elements [1] up to 1.55 W for 19 elements due to significantly improved heat sinking. The extracted power densities spatially averaged over the area close to the honeycomb like array arrangement raised from 0.33 kW/cm² to 1.25 kW/cm².

1. Introduction

Small diameter VCSELs are accepted devices for datacom applications due to their distinguished performance. One of those is the high conversion efficiency of more than 40 % which is also a basic for high-power devices. But most of the datacom VCSELs have output powers in the range of a few mW. For higher powers edge-emitting lasers are more suited because they achieve up to several W at high conversion efficiencies [2],[3]. Disadvantages of these devices are the strongly elliptical beam with a large divergent far-field angle in the fast axis and the high effort in testing and mounting. To close the gap between low power datacom VCSELs and high power edge-emitting lasers large-area single device VCSELs [4] and two-dimensional arrays [5] have been investigated. More than 2 W at -1°C heat sink temperature are reported from a VCSEL array consisting of a large number of 1000 single elements resulting in a chip area averaged power density of 30 W/cm². Our aim is to fabricate devices which combine high optical output powers in the Watt regime, high conversion efficiencies above 20 % and high power densities of more than 1 kW/cm² in cw-operation at room temperature. Therefore a layout with high packing densities and optimized number of elements is performed. As carried out in this previous work [1], large-area top-emitting VCSELs are not suited because of the decreasing efficiencies with increasing device size and the poor beam quality due to the ring-shaped near field caused by the inhomogeneous carrier injection through the top ring contact. Therefore we have concentrated the work on bottom-emitting devices which provide a homogeneous current injection also for large-area devices and are suited for a sophisticated mounting technique.

2. Device Structure

The fabrication of bottom-emitting single devices and two-dimensional arrays is very similar. The layer structure is grown by solid-source molecular beam epitaxy on GaAs-substrate. A schematic cross-sectional view of a VCSEL array is shown in Fig. 1. The

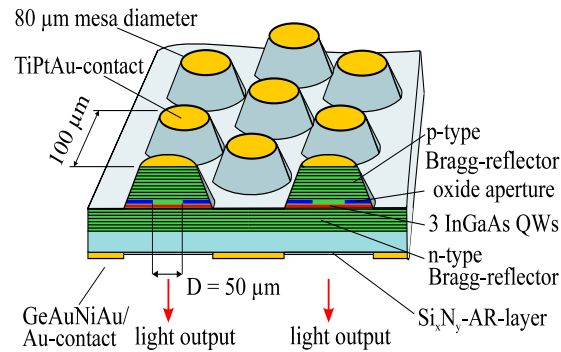


Fig. 1. Cross-sectional view of the oxidized VCSEL array.

carbon doped p-type Bragg reflector consists of 30 pairs of $\text{Al}_{0.9}\text{Ga}_{0.1}\text{As}/\text{GaAs}$ layers. The active region is composed of three 8 nm thick $\text{In}_{0.2}\text{Ga}_{0.8}\text{As}$ quantum wells for an emission wavelength of about 980 nm. Above the p-type cladding layer a 30 nm thick AlAs layer is inserted. Wet chemically etching with sulphuric acid is used to define mesa type active regions. The exposed AlAs layer is laterally oxidized in a water vapor atmosphere using nitrogen as carrier gas at a temperature of 410°C in order to form the current aperture and determine the active diameter of the device. For light emission through the GaAs substrate the silicon doped n-type distributed Bragg reflector has only 20 layer pairs of the same composition as the p-type mirror. On top of the mesa a full size p-contact consisting of Ti/Pt/Au is evaporated which provides a homogeneous current distribution and serves as a wettable metal pad for soldering. After mechanically polishing the GaAs substrate down to a thickness of 150 μm , an anti-reflection coating of Si_3N_4 with refractive index of 1.89 and quarter-wavelength thickness is deposited using plasma enhanced chemical vapor deposition. The Si_3N_4 layer is opened selectively with reactive ion etching for Ge/Au/Ni/Au large-area contacts surrounding the emission windows. After annealing the n-type contact at 400°C the processing is completed by depositing an electroplated Au layer of 1-2 μm thickness.

3. Mounting on Heat Sinks

VCSELs with active diameters up to 100 μm can be operated without mounting on heat sinks and are generally capable for on-wafer-testing of electro-optical device performance like threshold current density, threshold voltage, differential resistance, differential efficiency and emission wavelength. Due to a slight gradient in layer thickness across the grown wafer and corresponding detuning of gain and cavity resonance device performance

depends on wafer position. Only large active diameter VCSELs with matched gain and cavity resonance are suited for highest output powers since not optimized detuning increases threshold current and dissipated power drastically. On-wafer-tests are performed in order to select appropriate large-area devices or arrays for mounting. The standard mounting technique shown in Fig. 2 is the same for single devices and for two-dimensional arrays.

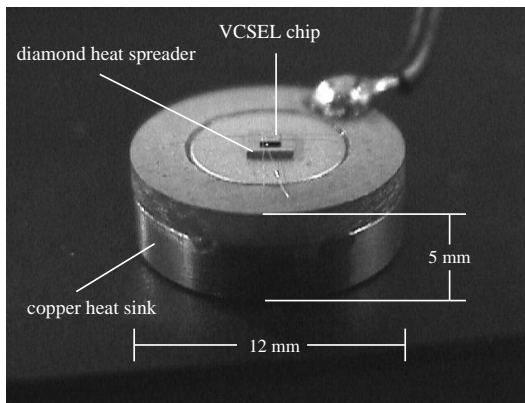


Fig. 2. Mounted semiconductor chip on metallized diamond and copper heat sink.

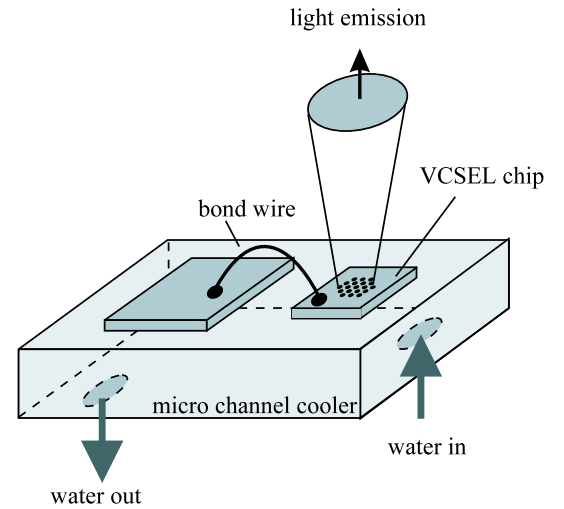


Fig. 3. Schematic drawing of a mounted semiconductor chip on a water cooled copper submount.

The cleaved semiconductor chip with dimensions between $0.5 \times 0.5 \text{ mm}^2$ (single device) and $0.8 \times 0.8 \text{ mm}^2$ (two-dimensional arrays) is soldered junction-down with eutectic $\text{Au}_{80}\text{Sn}_{20}$ -solder on a metallized diamond heat spreader of $2 \times 2 \text{ mm}^2$ size. The same AuSn solder is used to attach the diamond on a small copper heat sink. Soldering is achieved in a single-step heating process at a temperature of about 300°C . The cylindrical copper mount has a diameter of 12 mm and a height of 5 mm. In the backside a thread is cut for easy mounting on a larger heat sink. Heat dissipation predominantly occurs through the p-type contact. For the two-dimensional arrays the p-contact is common for all devices after mounting. Therefore a good homogeneity of the electrical parameters for all devices across the array is required.

As an alternative heat sink a microchannel cooler has also been employed for two-dimensional arrays as indicated in Fig. 3. The thickness of the water cooled copper-plate where the array is soldered onto is about 0.4 mm and the thickness of the indium solder is about $3 \mu\text{m}$. To reduce costs the semiconductor chip is mounted without diamond heat spreader. The thermal strain on the devices during soldering is reduced because the melting point of indium is only about 160° . Both solders are generally applied and tested for high-power edge-emitting lasers. The mounting can be done automatically by pick-and-place machines because alignment tolerances are much more relaxed compared to edge-emitting lasers. The electrical connections are done via wire-bonding.

4. Large-Area Single Devices

In Fig. 4 the output characteristics for 3 different device sizes of 170, 245 and 320 μm are shown. The threshold currents are 215 mA, 465 mA and 1.1 A, respectively. This corresponds to a threshold current density of 1 kA/cm^2 . The maximum output powers are 450 mW, 740 mW and 890 mW. The highest value we have obtained before was 350 mW for a device with 200 μm active diameter [6]. In comparison to these results, the mounting technique has improved drastically. Various applications like free space data transmission, optical sensing or LIDAR request pulsed operation. Therefore the capability of the largest device has been investigated. The electrical pulses had a width of approximately 10 ns and a repetition rate of 67 kHz. The optical pulses for different laser currents are slightly wider as can be seen in Fig. 5 due to reflections in the supply cables between the current source and the laser.

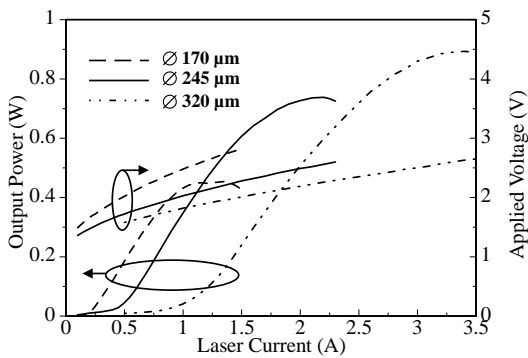


Fig. 4. Output characteristics for large-area single devices with 170, 245 and 320 μm active diameter.

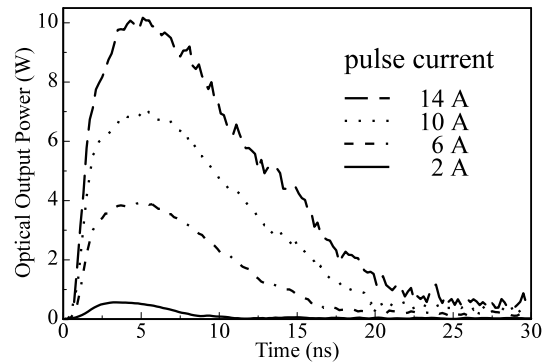


Fig. 5. Optical pulses measured by a fast photodiode at different laser currents. The width of the electrical pulses was about 10 ns and the repetition rate 67 kHz.

The maximum peak output power of 10 W is achieved at a current of 14 A which was the limit of the current source. At this point a current density of 17.5 kA/cm^2 is present and there are still no thermal effects observable.

In VCSELs with small active diameters of around 5 μm current densities at thermal rollover of more than 50 kA/cm^2 are applied so peak output powers in the range of 30 W seem to be possible.

Due to the large active diameter the emitted light is strongly multi-mode. To measure the spectrum of these VCSELs one has to ensure that all light is detected in a spectrum analyzer. Therefore the coupling into a small core diameter fiber of e.g. 50 μm is not reasonable because mode filtering would occur. To avoid errors in measuring we coupled the light into a 600 μm core diameter silica fiber with a numerical aperture of 0.37. The disadvantage of this setup is the low resolution of the analyzer which is about 0.5 nm. The mode spacing is in the range of a few picometer so single modes can not be observed

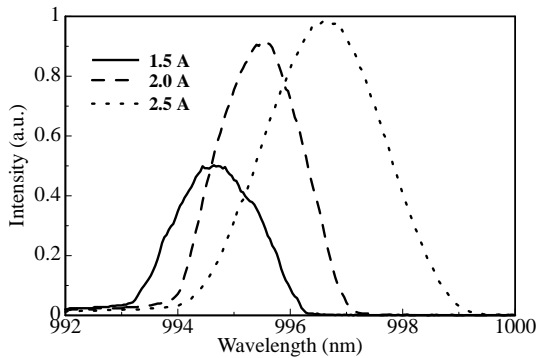


Fig. 6. Spectra of the 320 μm active device for different laser currents.

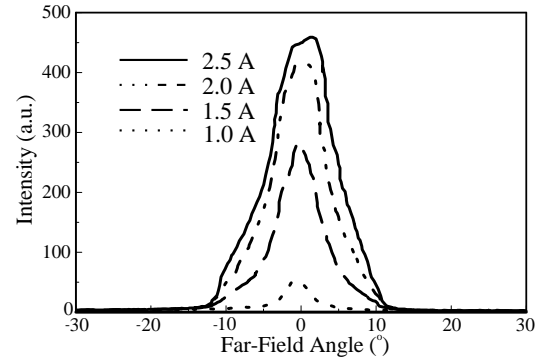


Fig. 7. Far-field measurements of the 320 μm active device for different laser currents.

and the shape of the spectrum is smooth in comparison to small VCSELs as can be seen in Fig. 6. The peak-wavelength is in the range of 995 nm due to the cavity resonance which can be designed for wavelengths between 940 nm and 1020 nm by changing the thickness of the DBR layer pairs. The full width at half maximum of the spectra is lower than 5 nm for all currents which is useful for applications like pumping of Er- or Yb-doped fibers and Nd-YAG microdisk lasers. The far-field of this laser is shown in Fig. 7 again for different laser currents. The graph shows a single lobe with a FWHM of less than 12° for all currents and no side-lobes or amplified spontaneous emission (ASE) are observed. Due to the circularly symmetric far-field pattern the beam can easily be focused or collimated by one usual lens. In comparison to edge-emitting lasers the low divergent beam is astigmatism free and shows no filamentations.

5. Two-Dimensional VCSEL Arrays

Criteria for optimized array design were discussed in previous works [1],[7]. First arrays consisted of 23 elements with active diameters between 30 - 40 μm and center-to-center spacings between 70 - 90 μm . For an active diameter of 40 μm and a spacing of 90 μm this results in maximum output powers of 0.56 W in cw-operation at room temperature and 0.8 W at -10°C . The corresponding power densities spatially averaged over the cleaved semiconductor chip are 0.33 and 0.47 kW/cm^2 , respectively. In order to obtain maximum optical output power at high power densities, the number of elements was first reduced to 19 individual devices again arranged in a honeycomb-like layout with a mesa diameter of 80 μm and an active diameter of 40 μm defined by oxidation of the current aperture. The center-to-center spacing of neighboring elements is 100 μm and the area close to the honeycomb-like arrangement of the lasers is about 0.123 mm^2 as can be seen in Fig. 8 from the white line. The array was soldered on a microchannel cooler as shown in Fig. 3 and tested in cw-operation at 18°C water temperature. Due to the fact that all devices are driven in parallel after mounting the threshold current is 285 mA which corresponds to 19 times the threshold of a single device. The maximum output power is 0.97 W which

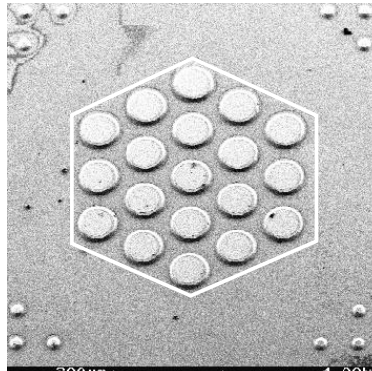


Fig. 8. Top view of the array with wet chemically etched mesas. The white line is drawn to indicate the effective area of the array.

corresponds to a spatially averaged power density of 0.81 kW/cm^2 over the effective chip area shown in Fig. 8 [8].

After optimization of the mounting technique and heat sinks, the active diameter was increased to $50 \mu\text{m}$ in order to increase the maximum output power and the array were mounted on both kinds of heat sinks, diamond heat spreader combined with a copper heat sink as well as microchannel cooler.

The differential resistance of the arrays with $50 \mu\text{m}$ active diameter mounted on diamond heat spreader combined with a copper heat sink is reduced to 0.48Ω which, due to some additional ohmic losses caused by the soldering, is slightly above the value expected for the given parallel connection. Fig. 9 shows the output characteristics of the array at different heat sink temperatures. The threshold current is decreased for lower temperatures indicating a slightly negative detuning of the gain peak with respect to the cavity resonance at room temperature. Maximum output power is as high as 1.08 W for a heat sink temperature of 18°C and increases to 1.4 W at 10°C . The maximum cw power density at 10°C exceeds 1 kW/cm^2 if a spatial average is taken over the area close to the honeycomb-like arrangement as indicated in Fig. 8. Maximum conversion efficiencies are above 20% over the whole temperature range with corresponding optical output powers between 0.6 W for 18°C and 0.8 W for 10°C .

The LIV-characteristics of an array mounted on the water cooled heat sink is given in Fig. 10. The water temperature again is 18°C and the maximum output power is as high as 1.55 W which corresponds to a power density of 1.25 kW/cm^2 . The higher output power in comparison to the array described above is mainly due to a better heat-sinking and heat removal by the water cooled submount.

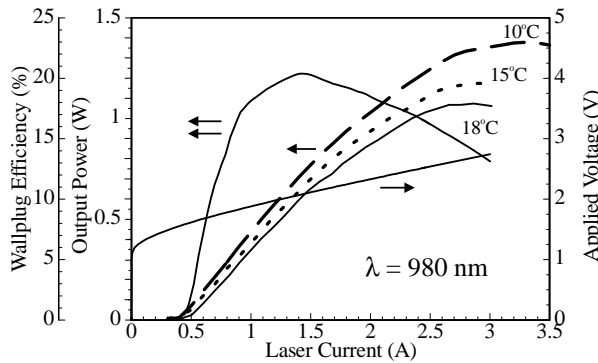


Fig. 9. Output characteristics of the mounted array under cw operation at different heat sink temperatures.

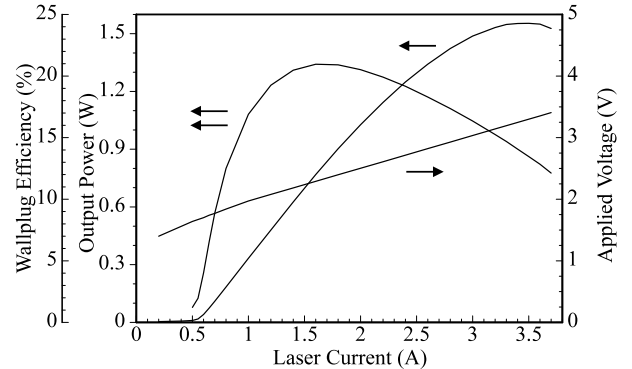


Fig. 10. LIV-characteristics and wallplug efficiency of a VCSEL array with active diameters of $50 \mu\text{m}$ mounted on a water cooled heat sink.

Since both arrays are from the same wafer and have similar electro-optical characteristics from on-wafer testing the output power is only depending on the mounting. This is also obvious from a simulation of the output characteristics. The calculated thermal conductivities λ_c of the modules achieved from a model, which is rather simple and described in detail in [1], are $320 \text{ W}/(\text{K}\cdot\text{m})$ for the diamond/copper-submount and $400 \text{ W}/(\text{K}\cdot\text{m})$ for the water cooled submount. This value is 8, respectively 10 times higher compared to devices with AlGaAs-material compositions tested on wafer without heat-sinking. A detailed study of the thermal properties has to be done in future with FEM-simulations.

6. Conclusion

In conclusion we have fabricated high-power VCSELs, single devices as well as two-dimensional arrays with proven potential for applications requiring output power in the Watt-regime. The single devices with active diameters up to $320 \mu\text{m}$ show output powers up to 0.89 W which is up to now the highest value reported. The arrays consisting of 19 elements with an individual active diameter of $50 \mu\text{m}$ and a spacing of $100 \mu\text{m}$ which are arranged in a dense honeycomb pattern achieve output powers of 1.55 W corresponding to a spatially averaged power density of $1.25 \text{ kW}/\text{cm}^2$ over the effective array chip size. Favorable beam profiles with low divergence angles and a high reliability of over 10.000 hours are remarkable characteristics that recommend for the implementation of VCSELs as high-power lasers. The wavelength is at the moment restricted between 900 and 1020 nm but further investigations in mounting and substrate removal will enable emission wavelengths down to about 800 nm where 808 nm is the desired pump wavelength for the Nd-YAG crystal. Future work is expected to result in modules with optical output powers of about 10 W in cw operation through increasing the number of elements and a further improved mounting technique.

References

- [1] M. Grabherr, M. Miller, R. Jäger, R. Michalzik, U. Martin, H. Unold, and K.J. Ebeling, “High-Power VCSEL’s: Single devices and densely packed 2-D-arrays,” *IEEE J. Select. Topics Quantum Electron.*, vol. 5, pp. 495–502, 1999.
- [2] A. Al-Muhanna, L.J. Mawst, D. Botez, D.Z. Garbuzov, R.U. Martinelli, and J.C. Connolly, “High-power (> 10 W) continuous-wave operation from 100- μ m-aperture 0.97- μ m-emitting Al-free diode lasers,” *Appl. Phys. Lett.*, vol. 73, pp. 1182–1184, 1998.
- [3] J. Braunstein, M. Mikulla, R. Kiefer, M. Walther, J. Jandeleit, W. Brandenburg, P. Loosen, R. Poprawe, and G. Weimann, “267 W cw AlGaAs/GaInAs Diode Laser Bars,” in *Laser Diodes and LEDs in Industrial, Measurement, Imaging, and Sensors Applications II; Testing, Packaging, and Reliability of Semiconductor Lasers V*, Proc. SPIE, vol. 3945, pp. 17-22, 2000.
- [4] F.H. Peters, M.G. Peters, D.B. Young, J.W. Scott, B.J. Thibeault, S.W. Corzine, and L.A. Coldren, “High power vertical-cavity surface-emitting lasers,” *Electron. Lett.*, vol. 29, pp. 200-201, 1993.
- [5] D. Francis, H.-L. Chen, W. Yuen, G. Li, and C. Chang-Hasnein, “Monolithic 2D-VCSEL array with 2 W CW and 5 W pulsed output power,” *Electron. Lett.*, vol. 34, pp. 2132-2133, 1998.
- [6] M. Grabherr, R. Jäger, M. Miller, C. Thalmaier, J. Heerlein, R. Michalzik, and K.J. Ebeling, “Bottom-Emitting VCSEL’s for high-cw optical output power,” *Photon. Technol. Lett.*, vol. 10, pp. 1061–1063, 1998.
- [7] M. Grabherr, M. Miller, R. Jäger, R. Rösch, U. Martin, H. Unold, and K.J. Ebeling, “Densely Packed High Power VCSEL Arrays,” in *Proc. ISLC 1998*, vol. 1, pp. 245–246, (Nara, Japan), Sep. 1998.
- [8] M. Grabherr, M. Miller, R. Jäger, and K.J. Ebeling, “Reliable 1 W cw VCSEL module for high optical power density,” in *Proc. LEOS Annual Meeting 1999*, vol. 1, pp. 265–266, (San Francisco, USA), Nov. 1999.